Available online at www.sciencedirect.com
ScienceDirect
Tetrahedron Letters
Tetrahedron Letters 48 (2007) 2791–2795

Design of molecular two-photon probes for in vivo imaging. 2*H*-Benzo[*h*]chromene-2-one derivatives

Hwan Myung Kim,[a] Xing Zhong Fang,[a] Pil Rye Yang,[a] Jae-Sung Yi,[b] Young-Gyu Ko,[b] Ming Jun Piao,[a] Young Dae Chung,[a] Young Woo Park,[a] Seung-Joon Jeon[a] and Bong Rae Cho[a,*]

[a]*Molecular Opto-Electronics Laboratory, Department of Chemistry, Korea University, 1-Anamdong, Seoul 136-701, Republic of Korea*
[b]*Graduate School of Life Sciences and Biotechnology, Korea University, 1-Anamdong, Seoul 136-701, Republic of Korea*

Received 24 January 2007; accepted 30 January 2007
Available online 14 February 2007

Abstract—2*H*-Benzo[*h*]chromene-2-one derivatives showing appreciable water solubility, significant two-photon cross sections, high photostability, cell permeability, low toxicity, and ability to be converted to a protein TP probe have been developed by incorporating all of the needed functions within a small molecule.

Two-photon microscopy (TPM) employing two NIR photons for the excitation is gaining much interest in biological imaging.[1] The advantages of TPM include improved three dimensional resolution due to the highly spatially localized excitation, increased penetration depth (~1000 μm), and lower tissue auto-fluorescence, as well as the reduced photodamage and photobleaching effects.[2] A useful TP probe for such applications should have significant TP cross section (δ_{TPA}), appreciable water solubility (>1 μM), cell permeability, high photostability, receptor for the metal ions or ability to be conjugated to the biomolecule, and low toxicity. Recent work has shown that TP fluorophores with large δ_{TPA}, appreciable water solubility, and enhanced photostability can be synthesized by optimizing the molecular structures.[3–5] Specifically, δ_{TPA} can be increased by using strong donor–acceptor groups while maintaining the planar structure to facilitate the intramolecular charge transfer (ICT),[3] water solubility by attaching solubilizing groups such as ammonium ions and oligo (ethylene glycol) monomethyl ether,[4] and photostability by enclosing the conjugating bridge within a heterocyclic ring, respectively.[5] Recently, TP probes sensitive to the metal ions, pH, and fluoride ion have been reported.[6,7] However, all of these have been studied either in organic solvents or in model membranes, not in the cells or tissues. Very recently, water soluble dendrimeric TP tracers (MW = ~30 kDa) have been developed for in vivo imaging.[8] Therefore, there is a need to develop efficient molecular TP probes for in vivo imaging.

An ideal approach to this problem would be to incorporate all of the required functions within a small molecule. Although this optimization procedure may somewhat decrease the δ_{TPA}, it may not cause a serious problem because TPM has been successfully applied to bioimaging using one-photon fluorescent probes based on fluorescein derivatives (δ_{TPA} <40 GM).[9] Accordingly, we have designed 2*H*-benzo[*h*]chromene-2-one derivatives (**1**–**3**) having strong donor–acceptor pairs in the cyclic planar framework to facilitate the ICT for the high δ_{TPA}, conjugated double bond within a cycle to enhance the photostability, an integral ester group(s) as the acceptor to increase the water solubility, and small MW for the cell permeability. The parent chrome ring system was first introduced by Gamer et al.[10] and its fluorescence properties were studied by Murata et al.[11] Herein, we report that **1**–**3** are useful TP fluorophores that meet all of the requirements as outlined above.

The compounds were synthesized by condensation between **C**–**E** and dimethyl malonate or methyl cyanoacetate (Scheme 1). To synthesize a protein probe **3c**,**3a** was hydrolyzed to afford the carboxylic acid derivative, which was then reacted with *N*-hydroxysuccinimide.

* Corresponding author. Tel.: +82 2 3290 3129; fax: +82 2 3290 3121; e-mail: chobr@korea.ac.kr

0040-4039/$ - see front matter © 2007 Elsevier Ltd. All rights reserved.
doi:10.1016/j.tetlet.2007.01.176

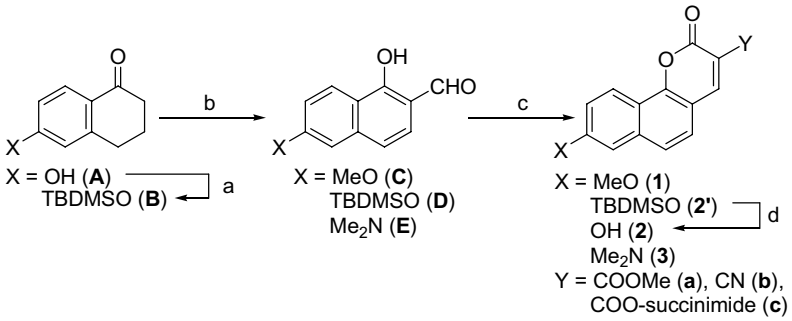

Scheme 1. Synthesis of **1**–**3**. Reagents and conditions:(a) TBDMSCl, imidazole, CH_2Cl_2; (b) (i) LDA, THF, −78 °C; (ii) HCO_2Et, −78 °C–rt, 24 h; (iii) DDQ, 1,4-dioxane, rt, 1 h; (c) $CH_2(CO_2Me)_2$ or $CNCH_2CO_2Me$, piperidinium acetate, toluene, reflux, 24 h; (d) TBAF, THF, 10 min.

All compounds show appreciable water solubility ($>1.0\times10^{-6}$ M) that is sufficient to stain the cells (Table 1). This indicates that our design strategy is efficient in providing water solubility without attaching a pendant solubilizing group. The solubility increases with the number of hydrogen bonding sites, that is, **1** ≈ **2** > **3**, although it is relatively insensitive to the change of the acceptor from COOMe (**3a**) to CN (**3b**).

The λ_{max} increases with the donor in the order, OMe < OH < Me_2N, and with the acceptor, that is, COOMe < CN (Table 1).

The fluorescence spectra show monotonous bathochromic shift with increasing donor–acceptor strength, that is, **1a** < **2a** < **3a** < **3b** (Fig. S2). The Stokes shifts are large, ranging from 4442 to 7040 cm^{-1} (Table 1). As the donor/acceptor strength increases, the charge transfer character of the excited electronic state would increase. This predicts that the solvation energy becomes large and the fluorescence Stokes shift will increase too. Interestingly, **2a** reveals two peaks, which are similar to those at pH 1.0 and 11.0 (Fig. S2). Moreover, the pK_a value of **2a** is approximately 7.3 (Supplementary data), indicating that the significant amount of **2a** would be deprotonated under neutral condition. Hence, the unusually large Stokes shift (7040 cm^{-1}) for **2a** can be attribute to the enhanced ICT in the excited state due to the much stronger donor ability of O^- than OH ($\sigma^+ = -2.3$ for O^- vs −0.91 for OH).[12]

The two-photon cross sections of **1**–**3** were measured in water solution by using the fluorescence measurement method using fluorescein (8×10^{-5} M in water, pH 11) as the reference, whose two-photon property has been well characterized in the literature.[3b,i,13] The two-photon excitation spectra for **1**–**3** are displayed in Figure 1. The reported values are the average of two or more measurements. The experimental uncertainty on δ_{TPA} is of the order of 10–15%.

Figure S4 shows that the one- and two-photon absorption maxima for **3a** show reasonable overlap in terms of the total absorption energy. This is consistent with the prediction that the two-photon allowed state of a dipolar molecule should be close to the Franck–Condon state.[14] Similar result was observed for all compounds, although we cannot rule out the possibility that the real

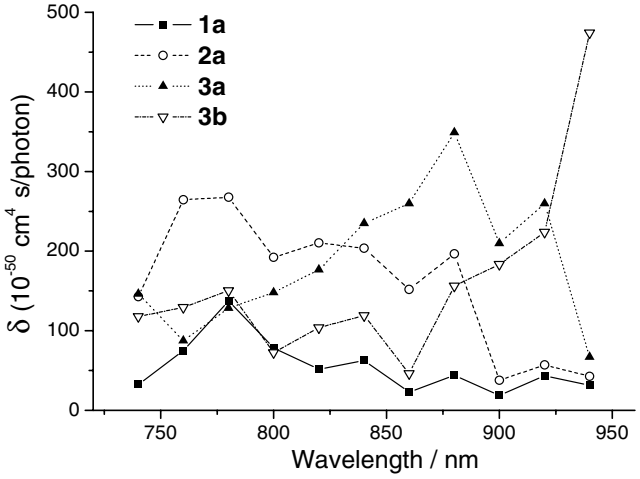

Figure 1. Two-photon excitation spectra of **1**–**3** in H_2O.

Table 1. Photophysical data for **1**–**3**

Cpd[a]	$\lambda_{max}^{(1)}$ [10^{-4} ε]	λ_{max}^{fl}	Δv[b]	Φ[c]	$\lambda_{max}^{(2)}$[d]	δ_{max}[e]
1a	391(1.99)	481	4785	0.82	780	140
2a[f]	397(1.37)	482, 551	4442, 7040	0.48	780	270
3a	453(1.54)	570	4531	0.19	880	350
3b	457(2.28)	590	4933	0.050	940	470

[a] Solubility in water for **1a**, **2a**, **3a**, and **3b** are 2.5×10^{-6}, 2.5×10^{-6}, 1.2×10^{-6}, and 1.0×10^{-6} M, respectively.
[b] Stokes shift in cm^{-1}.
[c] Fluorescence quantum yield.
[d] λ_{max} of the two-photon excitation spectra in nm.
[e] The peak two-photon absorptivity in 10^{-50} cm^4 s/photon (GM). The experimental uncertainty is of the order of 10–15%.
[f] The $\lambda_{max}^{(1)}$ and λ_{max}^{fl} of **2a** at pH 1 are 392 and 484 nm, and those at pH 11 are 433 and 553 nm, respectively.

$\lambda_{max}^{(2)}$ for **3b** may exist at a longer wavelength (Fig. 1). Interestingly, $\lambda_{max}^{(2)}$ of **1**–**3** appear at 780–940 nm in H_2O. This turns out to be important for biological imaging because most of TPM uses excitation wavelength in the range of 700–1000 nm. Moreover, the one- and two-photon excited fluorescence (TPEF) spectra overlap almost completely (Fig. S4). This indicates that the emission occurs from the same states, regardless of the mode of excitation.

The δ_{max} values of **1**–**3** are in the range of 140–470 GM and increase gradually with the donor/acceptor strength in the order, **1a** < **2a** < **3a** < **3b**, reaching at the maximum of 470 GM for **3b** (Table 1). A stronger donor/acceptor would not only increase the charge transfer character to further increase the TPA transition dipole matrix element, but also decrease the energy gap between the ground and first excited state as found in the monotonic red shift of the fluorescence spectrum. A combination of these effects would be to increase the δ_{max}.[3d,e]

Photostability was determined by using **3a**-labeled giant unilamellar vesicles (GUVs) grown from 1,2-dioleoyl-*sn*-glycero-3-phosphocholine (DOPC) phospholipids.[5] Photostability has been usually measured by the changes of the absorption and/or emission spectra of the probe in solution upon repetitive laser irradiation. However, it is not a direct measure of the photostability under the imaging condition because the dye molecules in solution can easily diffuse away from the focal point during the irradiation. To avoid such problems, we have monitored the TPEF intensity with time of the dyes loaded in the GUVs where the diffusion rate is much slower. The GUVs grown from DOPC have been used as the model for the cytosol because it is the most hydrophilic vesicle.

Figure 2a shows that the DOPC GUVs loaded with **3a** emit intense TPEF throughout the equatorial sections of GUVs when excited by the polarized light, indicating no photoselection effect. This reveals that the dye is easily loaded and randomly oriented in the GUVs.[15] Similar result is observed for 1,4-bis[(*E*)-4-(dihexylamino)styryl]benzonitrile (**4**) and 2,5-bis[6-(dihexylamino)-1-*H*-indole-2-yl]benzonitrile (**5**), except that the images are less clear indicating lower dye contents due to the limited water solubility (Fig. S5).[5] The TPEF intensity from the dye-loaded GUVs (~40 μm) decreased with irradiation time under TPM. As expected, the photobleaching rates follow 1st order kinetics,[5,16] with half lives ($t_{1/2}$) of 7.3, 14.5, and 108 min for **4**, and **5**, and **3a**, respectively (Fig. 2b). The 2-fold larger $t_{1/2}$ of **5** than **4** is in excellent agreement with our previous result determined in DPPC GUVs, and can be attributed to the lower photoreactivity of the aromatic C=C bond in the indoline moiety than the stilbenoid C=C bond in **4**.[5,16,17] Most interestingly, the $t_{1/2}$ of **3a** is larger than **5** by a factor of 8. The origin of this high photostability is not clear. However, the two acceptor groups at the C-3 of **3a** may have further stabilized the C=C bond and reduced the photoreactivity. Moreover, photochemically inert ester groups may have provided additional contribution.

To determine the cell permeability, A431 cells were washed with serum-free media and incubated with 5 μM of **3a** in serum-free media for 3 h at 37 °C. Figure 3a shows the TPEF image of **3a**-labeled A431 cells. The image is bright, indicating that **3a** can readily permeate through the cell membrane and the TPEF intensity is strong enough for TPM. Furthermore, we have investigated the internalization of a protein into the mammalian cells by using **3c** as the protein probe. For this experiment, we have used proinflammatory cytokine p43 protein, which is known to internalize into the bovine aorta endothelial cells (BAECs) after binding to the cell surface.[18] As shown in Figure S6, **3c** was easily conjugated to p43. When **3c**-conjugated p43 was incubated with BAECs at 37 °C, **3c**-conjugated p43 was internalized and accumulated within the cells as shown in Figure 3b. To the best of our knowledge, **3c** is the first TP protein probe developed by a rational design.

Finally, the toxicity of **3a** was determined by comparing the survival rates of the A431 cells labeled with **3a** or DMSO. The MTT assay result indicates negligible toxicity that is sufficient for the live cell imaging (Fig. S7).

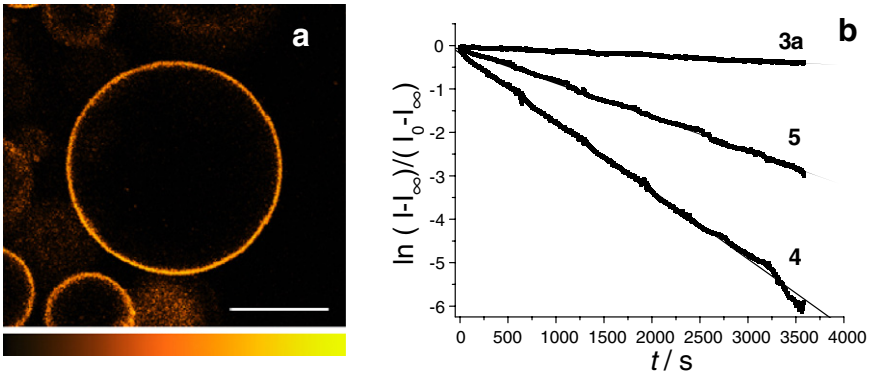

Figure 2. (a) Two-photon fluorescence image of **3a**-labeled GUVs composed of DOPC at 25.0 °C. The excitation light ($\lambda = 840$ nm) is polarized parallel to the horizontal axis of the image. The scale bar equals 20 μm; (b) Bleaching rates of TPEF in GUVs labeled with **3a**, **4**, and **5**. The thick lines are experimental data and the thin lines are first-order plots.

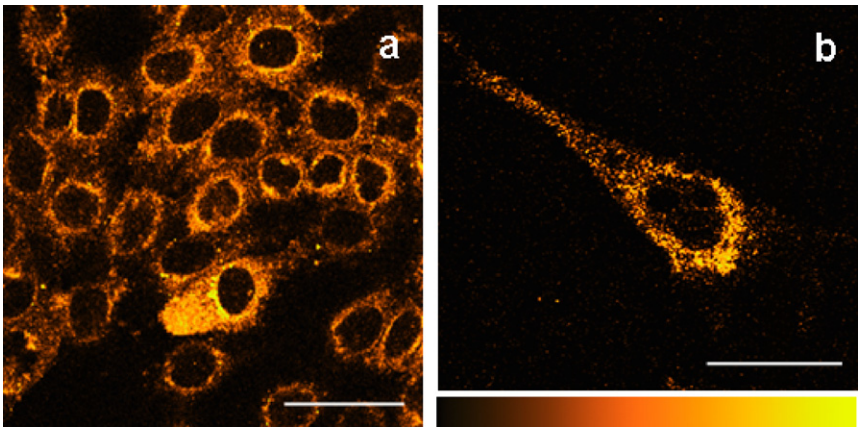

Figure 3. (a) Two-photon fluorescence images of **3a**-labeled A431 cells and (b) **3c**-conjugated p43 in bovine aorta endothelial cells. Excitation light $\lambda =$ (a) 880 nm, (b) 840 nm. The scale bar equals 30 μm.

In summary, we have developed useful TP fluorophores that show appreciable water solubility, significant δ_{TPA}, high photostability, cell permeability, low toxicity, and that can easily be converted to a TP protein probe by incorporating all of the needed functions within a small molecule. This result will provide a useful guideline for the design of efficient molecular TP probes for in vivo imaging.

Acknowledgment

This work was supported by KOSEF (2006-03792) and CRM-KOSEF.

Supplementary data

Synthesis of **1**–**3**, solubility measurements, photophysical studies, vesicle and cell preparation, conjugation of **3c** to p43 protein, two-photon imaging, and MTT assay are available as Supplementary data and can be found, in the online version, at doi:10.1016/j.tetlet.2007.01.176.

References and notes

1. (a) Denk, W.; Strickler, J. H.; Webb, W. W. *Science* **1990**, *248*, 73; (b) Zipfel, W. R.; Williams, R. M.; Webb, W. W. *Nat. Biotechnol.* **2003**, *21*, 1369.
2. So, P. T. C.; Dong, C. Y.; Masters, B. R.; Berland, K. M. *Annu. Rev. Biomed. Eng.* **2000**, *2*, 399.
3. (a) Chung, S.-J.; Kim, K.-S.; Lin, T.-C.; He, G. S.; Swiatkiewicz, J.; Prasad, P. N. *J. Phys. Chem. B* **1999**, *103*, 10741; (b) Rumi, M.; Ehrlich, J. E.; Heikal, A. A.; Perry, J. W.; Barlow, S.; Hu, Z.; McCord-Maughon, D.; Parker, T. C.; Röckel, H.; Thayumanavan, S.; Marder, S. R.; Beljonne, D.; Brédas, J.-L. *J. Am. Chem. Soc.* **2000**, *122*, 9500; (c) Ventelon, L.; Charier, S.; Moreaux, L.; Mertz, J.; Blanchard-Desce, M. *Angew. Chem., Int. Ed.* **2001**, *40*, 2098; (d) Cho, B. R.; Son, K. H.; Lee, S. H.; Song, Y.-S.; Lee, Y.-K.; Jeon, S.-J.; Choi, J. H.; Lee, H.; Cho, M. *J. Am. Chem. Soc.* **2001**, *123*, 10039; (e) Lee, W.-H.; Lee, H.; Kim, J.-A.; Choi, J.-H.; Cho, M.; Jeon, S.-J.; Cho, B. R. *J. Am. Chem. Soc.* **2001**, *123*, 10658; (f) Yoo, J.; Yang, S. K.; Jeong, M.-Y.; Ahn, H. C.; Jeon, S.-J.; Cho, B. R. *Org. Lett.* **2003**, *5*, 645; (g) Porrès, L.; Mongin, O.; Katan, C.; Charlot, M.; Pons, T.; Mertz, J.; Blanchard-Desce, M. *Org. Lett.* **2004**, *6*, 47; (h) Chung, S.-J.; Rumi, M.; Alain, V.; Barlow, S.; Perry, J. W.; Marder, S. R. *J. Am. Chem. Soc.* **2005**, *127*, 10844; (i) Lee, S. K.; Yang, W. J.; Choi, J. J.; Kim, C. H.; Jeon, S.-J.; Cho, B. R. *Org. Lett.* **2005**, *7*, 323; (j) Yang, W. J.; Kim, D. Y.; Jeong, M.-Y.; Kim, H. M.; Lee, Y. K.; Fang, X.; Jeon, S.-J.; Cho, B. R. *Chem. Eur. J.* **2005**, *11*, 4191; (k) Ahn, T. K.; Kim, K. S.; Kim, D. Y.; Noh, S. B.; Aratani, N.; Ikeda, C.; Osuka, A.; Kim, D. *J. Am. Chem. Soc.* **2006**, *128*, 1700.
4. (a) Woo, H. Y.; Hong, J. W.; Mikhailovsky, B.; Liu, A.; Korystov, D.; Bazan, G. C. *J. Am. Chem. Soc.* **2005**, *127*, 820; (b) Woo, H. Y.; Korystov, D.; Mikhailovsky, A.; Nguyen, T.-Q.; Bazan, G. C. *J. Am. Chem. Soc.* **2005**, *127*, 13794; (c) Hayek, A.; Bolze, F.; Nicoud, J.-F.; Baldeck, P. L.; Mély, Y. *Photochem. Photobiol. Sci.* **2006**, *5*, 102.
5. Kim, H. M.; Yang, W. J.; Kim, C. H.; Park, W.-H.; Jeon, S.-J.; Cho, B. R. *Chem. Eur. J.* **2005**, *11*, 6386.
6. (a) Kim, H. M.; Jeong, M.-Y.; Ahn, H. C.; Jeon, S.-J.; Cho, B. R. *J. Org. Chem.* **2004**, *69*, 5749; (b) Pond, J. K. J.; Tsutsumi, O.; Rumi, M.; Kwon, O.; Zojer, E.; Brédas, J.-L.; Marder, S. R.; Perry, J. W. *J. Am. Chem. Soc.* **2004**, *126*, 9291; (c) Ahn, H. C.; Yang, S. K.; Kim, H. M.; Li, S.; Jeon, S.-J.; Cho, B. R. *Chem. Phys. Lett.* **2005**, *410*, 312.
7. (a) Werts, M. H. V.; Gmouh, S.; Mongin, O.; Pons, T.; Blanchard-Desce, M. *J. Am. Chem. Soc.* **2004**, *126*, 16294; (b) Liu, Z.-Q.; Shi, M.; Li, F.-Y.; Fang, Q.; Chen, Z.-H.; Yi, T.; Huang, C.-H. *Org. Lett.* **2005**, *7*, 5481.
8. Krishna, T. R.; Parent, M.; Werts, M. H. V.; Moreaux, L.; Gmouh, S.; Charpak, S.; Caminade, A.-M.; Majoral, J.-P.; Blanchard-Desce, M. *Angew. Chem., Int. Ed.* **2006**, *45*, 4645.
9. Euler, T.; Detwiller, P. B.; Denk, W. *Nature* **2002**, *418*, 845.
10. Cramer, F.; Windel, H. *Chem. Ber.* **1956**, *89*, 354.
11. Murata, C.; Masuda, T.; Kamochi, Y.; Todoroki, K.; Yoshida, H.; Nohta, H.; Yamaguchi, M.; Takadate, A. *Chem. Pharm. Bull.* **2005**, *53*, 750.
12. Hines, J. *Structural Effects on Equilibria in Organic Chemistry*; John & Wiley: New York, 1975; pp 66–72.
13. Xu, C.; Webb, W. W. *J. Opt. Soc. Am. B.* **1996**, *13*, 481.
14. McClain, W. M. *Acc. Chem. Res.* **1974**, *7*, 129.
15. Krasnowska, E. K.; Gratton, E.; Parasassi, T. *Biophys. J.* **1998**, *74*, 1984.
16. Giloh, H.; Sedat, J. W. *Science* **1982**, *217*, 1252.

17. (a) Belfield, K. D.; Bondar, M. V.; Przhonska, O. V.; Schafer, K. J. *J. Photochem. Photobiol. A* **2004**, *162*, 489; (b) Belfield, K. D.; Bondar, M. V.; Przhonska, O. V.; Schafer, K. J. *Photochem. Photobiol. Sci* **2004**, *3*, 138; (c) Grynkiewicz, G.; Poenie, M.; Tsien, R. Y. *J. Biol. Chem.* **1985**, *260*, 3440.

18. (a) Ko, Y.-G.; Park, H.; Kim, T.; Lee, J.-W.; Park, S. G.; Seol, W.; Kim, J. E.; Lee, W.-H.; Kim, S. H.; Park, J.-E.; Kim, S. *J. Biol. Chem.* **2001**, *276*, 23028; (b) Yi, J.-S.; Lee, J.-Y.; Chi, S.-G.; Kim, J.-H.; Park, S. G.; Kim, S.; Ko, Y.-G. *J. Cell. Biochem.* **2005**, *96*, 1286.